JOURNAL OF MATERIALS SCIENCE **40** (2005) 4009–4017

# Effects of density and strain rate on properties of syntactic foams

E. WOLDESENBET*
*Mechanical Engineering Department, Southern University, Baton Rouge, LA 70813, USA*
*E-mail: woldesen@me.lsu.edu*

NIKHIL GUPTA
*Mechanical, Aerospace and Manufacturing Engineering Department, Polytechnic University, Brooklyn, NY 11201, USA*

A. JADHAV
*Mechanical Engineering Department, Louisiana State University, Baton Rouge, LA 70803, USA*

Syntactic foams are characterized for high strain rate compressive properties using Split-Hopkinson Pressure Bar (SHPB) technique in this study. The results at high strain rates are compared to quasi-static strain rate compressive properties of the same material. Four different types of syntactic foams are fabricated with the same matrix resin system but different size microballoons for testing purpose. The microballoons have the same outer radius. However, their internal radius is different leading to a difference in their density and strength. The volume fraction of the microballoons in syntactic foams is maintained at 0.65. Such an approach is helpful in isolating and identifying the contribution of matrix and microballoons to the dynamic compressive properties of syntactic foams. Results demonstrate considerable increase in peak strength of syntactic foams for higher strain rates and increasing density. It is also observed that the elastic modulus increases with increasing strain rate and density. Scanning electron microscopy is carried out to understand the fracture modes of these materials and the density effect on high strain rate properties of syntactic foam. 

## 1. Introduction

High damage tolerance, low density and high specific strength of open and close cell structured foams make them suitable for aeronautical and marine structural applications [1, 2]. Normally open cell foams have lower density and strength compared to close cell structured foams. However, moisture absorption and thermal expansion coefficients of close cell foams are lower [3, 4]. Depending on loading and environmental conditions either open or close cell structured foams can be selected for a specific application. Both foams are widely used in sandwich composites as core materials [5].

Syntactic foams are one of the most widely used close cell structured foams. These foams are fabricated by incorporation of hollow particles (microballoons) in a matrix material. Such kind of foams give great design flexibility as microballoons and matrix can be made up of any material depending on the desired composite properties. Volume fraction of constituents and interfacial properties can also be adjusted to fabricate syntactic foams exactly as per requirements. Quasi-static properties of syntactic foams can be found studied in the literature particularly. Large numbers of studies on compressive properties of these materials are published in the literature [6–13]. These studies characterize the stress-strain behavior, the energy absorption characteristics and the fracture features of various types of polymer matrix syntactic foams. A stress plateau region observed in the stress-strain graphs of syntactic foams is found to be of particular interest because it represents the energy absorption characteristics of the foams.

Large number of studies can be found in the published literature on the high strain rate testing of various kinds of polymeric and metallic foams performed by using various techniques. Dynamic tests are conducted in industry to characterize the impact energy behavior of a variety of rigid polymers using drop weight tower [14] or simulated head impact using dynamic impact sled [15]. High strain rate mechanical properties of metallic foams have been studied by many researchers using the Split Hopkinson Pressure Bar (SHPB) technique [16–19]. These studies suggest that compressive

* Author to whom all correspondence should be addressed.

flow stress of the Al-foam is a function of the relative density but does not exhibit strain rate sensitivity. High strain rate compressive behavior of a rigid polyurethane foam with various densities is determined by Chen et. al [20]. They found the peak stress to be strain rate sensitive and expressed it in terms of the square of the foam density. Tensile and compressive properties of polystyrene bead (PSB) foams at various temperatures and strain rates are studied extensively by Rinde *et al*. [21]. Some of the previous studies on the dynamic properties of honeycomb structures can also be found in the published literature [22, 23]. These studies found an increase of 20 to 70% in the dynamic crush strength at impact velocities of 30 m/s. Some recent studies related to the high strain rate properties of syntactic foams can also be found published in recent times [24, 25]. These studies have tested one type of syntactic foam at a variety of strain rates between 300 and 1900 $s^{-1}$ and at different temperatures. However, comprehensive studies relating the properties of various constituting materials to the high strain rate properties of syntactic foams are needed.

Applications in aircraft and marine structure components require strong understanding of dynamic mechanical properties of syntactic foams because the impact loading conditions may significantly alter mechanical response of the material. Hence, syntactic foams should also be characterized for high strain rate properties by carefully controlled experiments. Such data are essential for conducting realistic numerical simulations for safe design of structures.

In the present work the high strain rate characterization of syntactic foams of four different densities but of the same microballoon volume fraction is conducted using a SHPB. Solid cylindrical specimens of aspect ratio (length/diameter) of 1 are used for the tests. The results of the high strain rate tests are subsequently compared to those of quasi-static tests. The effect of strain rate variation on the values of compressive strength, failure strain and compressive modulus is observed and analyzed. Extensive optical and scanning electron microscopic observations are performed to establish the high strain rate failure mechanisms in syntactic foams and relate them to the mechanical properties of the materials.

## 2. Syntactic foam structure

Syntactic foams are two-phase materials having microballoons dispersed in a matrix material. Structure of syntactic foams is shown in Fig. 1. It is possible to change the density of syntactic foams without changing the volume fractions of microballoons and matrix material in the structure. This can be achieved by selecting microballoons of different wall thicknesses. Another advantage of this approach is that a constant interfacial area between matrix and microballoons can be maintained while varying the density of the syntactic foam.

Microballoon wall thickness can be related to a parameter named Radius Ratio, $\eta$, which is given by Equation 1.

$$\eta = \frac{r_1}{r_0} \tag{1}$$

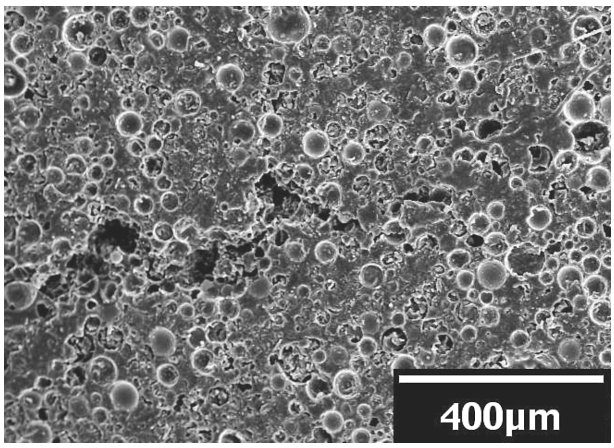


*Figure 1* Structure of a syntactic foam.

Where $r_1$ is the internal and $r_0$ is the outer radius of the microballoon. The parameter $\eta$ varies between 0 and 1. Increase in $\eta$ corresponds to a decrease in wall thickness, which leads to a decrease in true particle density of microballoon. Therefore, microballoons having higher $\eta$ value give rise to lower density syntactic foams and vice versa.

Microballoon can be divided into two categories based on their $\eta$ value. It is theoretically established that syntactic foams having $\eta$ value lower or higher than 0.71 experience different stress states in the specimens during compression testing [26]. All selected types of microballoons have $\eta$ value more than the critical value of 0.71 in order to make the direct comparison of experimental results meaningful.

## 3. Material preparation

### 3.1. Syntactic foam fabrication

Four types of microballoons, manufactured and supplied by 3M under the trade name "Scotchlite" are selected for the fabrication of syntactic foam specimens. All four types of microballoons have nearly identical mean outer radius, however, $\eta$ is different for each of them. The mean particle diameter and true particle density of selected microballoons, supplied by the manufacturer, are given in Table I. Diglycidylether of bisphenol A based epoxy resin D.E.R. 332 manufactured by DOW Chemicals with hardener D.E.H. 24 is used as the matrix material. A diluent $C_{12}$–$C_{14}$ aliphaticglycidylether is used to lower down the viscosity of the resin, which is desired to properly mix and wet microballoons. The volume fraction of microballoons is maintained at 0.65 in all types of syntactic foams.

TABLE I. Properties of microballoons used to fabricate syntactic foam slabs

| Microballoon type | Microballoon density ($kg/m^3$) | Mean microballoon diameter (µm) | Calculated radius ratio $\eta$ |
|---|---|---|---|
| S22 | 205 | 35 | 0.922 |
| S32 | 320 | 40 | 0.907 |
| S38 | 380 | 40 | 0.888 |
| K46 | 460 | 40 | 0.863 |

TABLE II. Density and void volume fractions in the fabricated syntactic foams

| Microballoon type | Corresponding foam nomenclature | Syntactic foam density (kg/m$^3$) | Void volume fraction (%) |
|---|---|---|---|
| S22 | SF 22 | 493 | 6 |
| S32 | SF 32 | 545 | 9 |
| S38 | SF 38 | 575 | 10 |
| K46 | SF 46 | 650 | 6 |

Fabrication of syntactic foams is carried out in a two-step process, i.e. mixing and casting. First the resin and diluent are mixed and heated to 50°C to further reduce the viscosity of the mix. Hardener is then added and stirred thoroughly, followed by microballoons addition. The mixture is stirred gently to minimize the damage to microballoons during the mixing process. The slurry like mixture is then cast in stainless steel molds of 230 $\times$ 230 $\times$ 13 mm$^3$ dimensions and cured for at least 36 h at room temperature. Cast foam slabs are removed from the molds and post cured at 100 $\pm$ 3°C for 3 h. The fabricated syntactic foams have some entrapped air due to mechanical mixing. This entrapped air is termed as voids. The measured density and the calculated void volume fraction values of fabricated syntactic foams are presented in Table II.

### 3.2. Test specimens

During high strain rate testing using the SHPB, specimen diameter never exceeds the pressure bar diameter up to its fracture strain because of small Poisson's Ratio of foams. The diameter of the samples is kept slightly less than that of the SHPB bars (9.65 mm). Cylindrical foam specimens of 9.5 mm in diameter and 9.5 mm in length are core drilled from the slabs for testing. The specimen ends of these core-drilled specimens are then carefully polished with 400-grit polish paper.

## 4. Testing methods

### 4.1. Static testing

Compression testing of the fabricated syntactic foams is carried out using MTS 810 Material Test System as shown in Fig. 2. Load and displacement data obtained from the machine is used for the calculation of compressive strength and modulus. Constant crosshead velocity of 1.3 mm/min was maintained as recommended by ASTM D 695–94 standard for such tests. This compression rate corresponds to a strain rate of about 0.0003 s$^{-1}$. Test specimens have cross section area of 25.4 $\times$ 12.5 mm$^2$ and height of 25.4 mm. Results of the static compression tests have been published elsewhere in detail [27].

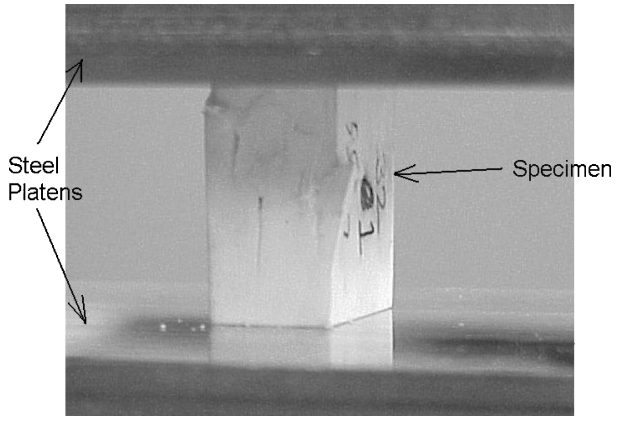


*Figure 2* Static compression testing setup of syntactic foam specimen.

### 4.2. High strain rate testing

#### *4.2.1. Testing procedure*

High strain rate tests are conducted using a compression type SHPB equipment that is popularly known as Kolsky bar well described in the literature [28, 29]. In this technique a cylindrical specimen is mounted between long incident and transmitter bars of very high yield strength while a short striker bar is used to produce an impact on one end of the incident bar. The overall specimen dimensions are required to be small enough to minimize the effects of longitudinal and lateral inertia and wave dispersion within the specimen. In addition, a frictional constraint at both pressure bar-specimen interfaces due to the radial expansion of the specimen during loading can produce non-uniform deformation in the specimen. These frictional constraints have been significantly reduced by applying a thin film of lubricant at the interfaces [29]. In the present study molybdenum disulphide lubricant is applied. The details about testing by using this technique for high strain rate testing of materials can be found elsewhere in the literature [29].

#### *4.2.2. Instrumental characterization*

High strain tests are carried out on a SHPB by varying the air pressure in the chamber from 60 to 250 psi to achieve striker bar velocities between 5 and 15 m/s. The stress wave produced initially undergoes distorting wave phenomenon contrary to the basic assumption of uniaxial wave propagation. The waves with narrower frequency bandwidth suffer less from distorting effects of dispersion. Such bandwidth can be obtained by increasing the rise time of the wave. Shaping of impact pulse is achieved by placing a yielding material (impact plenum) between the striker bar and the input bar. Mild steel plenum with 6.73 mm diameter is used in this experimental work.

A typical oscilloscope record for the materials under testing obtained from SHPB experiments is shown in Fig. 3. Waves for the incident and the transmitter bar can be observed in this figure. The first pulse, denoted by A, in the incident wave is incident pulse; whereas the second pulse (B) is reflected pulse. If the mechanical impendence of the specimen is less than that of the bar, the two pulses are opposite in sign, as shown in this figure. The transmitted pulse (C) through the syntactic foam specimen is lower in magnitude than the incident pulse A. In the last part of the transmitted pulse, its magnitude decreases gradually compared to the incident pulse in a way similar to metallic specimens

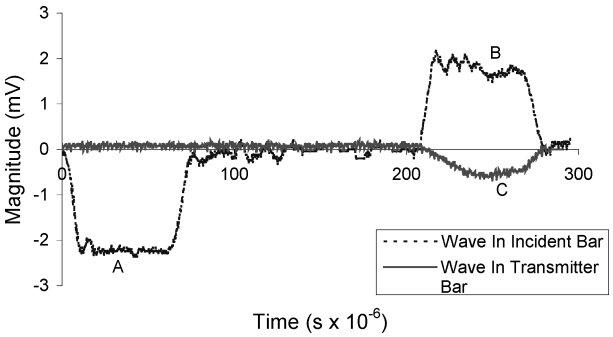


*Figure 3* Typical oscilloscopic record for high strain rate testing of syntactic foam specimens.

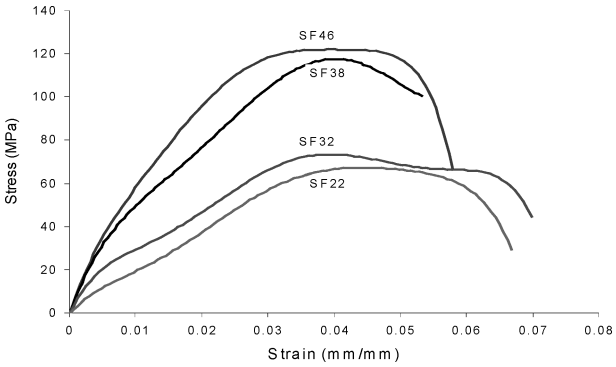


*Figure 5* Stress vs. Strain curves for syntactic foams of various densities at strain rates of around 1050 $s^{-1}$.

[30]. The transmitted pulse records the stress history in the specimen whereas the reflected pulse records the specimen strain rate and strain. By comparison of two pulses, B and C, it can be noted that the magnitude of the reflected pulse is very high compared to the transmitted pulse. It shows relatively higher amount of total strain at lower value of stress in comparison with other composite materials such as graphite/epoxy, which fail at relatively much lower strain [31]. The plateau in the reflected pulse indicates that the specimen deformed at a nearly constant strain rate for most part of the time during specimen deformation.

The strain rate for a given test varies as a function of time. Initially it increases from zero and remains relatively steady at a certain value as mentioned in the previous paragraph. The average strain rate value is obtained and used to characterize the specific experiment. Based on the assumption that the dynamic force in both the incident and transmitted bar are equal, the following equation can be written.

$$\varepsilon_T - \varepsilon_I = \varepsilon_R \tag{2}$$

where, $\varepsilon_T$, $\varepsilon_I$ and $\varepsilon_R$ are pressure bar strains due to transmitted, incident and reflected pulse, respectively. This verification of dynamic equilibrium is presented in Fig. 4. The two curves match with each other reasonably well.

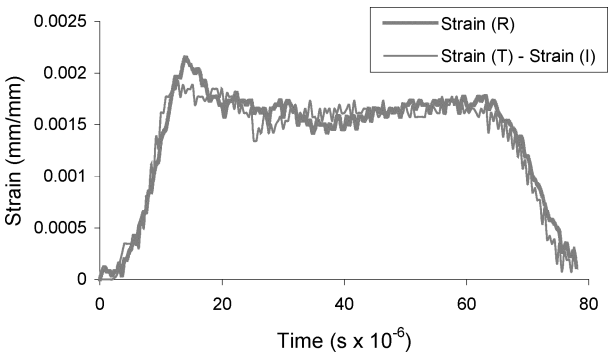


*Figure 4* Verification of equation of dynamic equilibrium for the high strain rate response.

## 5. Results and discussion

### 5.1. Stress-strain behavior

High strain rate compression test results of four types syntactic foams are discussed here to establish the effect of strain rate and effect of syntactic foam density on the dynamic compressive properties of syntactic foams. The results at high strain rates are compared to quasi-static strain rate compressive properties of the same material. Typical engineering stress versus engineering strain curves for various foam densities obtained at strain rates of approximately 1050 $s^{-1}$ are shown in Fig. 5. An almost linear initial region is found for each stress-strain curve where stress is directly proportional to strain up to about 3% strain. Another general observation for each of them is that the stress reaches to its peak value when the compressive strain is between 3.5 to 4%. The foam density is not found to influence the strain at peak stress value. This fact strongly indicates that the critical strain at which peak strength is observed does not depend on the type of microballoons and can be primarily recognized as the matrix property. Contrary to quasi-static stress-strain curves, the stress values do not drop drastically after maximum stress in high strain rate experiment. Only a small decrease in stress is observed after the peak stress value. After the peak, the stress stays nearly constant for increasing strain until it drops suddenly corresponding to the ultimate failure of the specimen. For some of the lower density specimens tested under dynamic conditions, stress oscillations are observed in this constant stress region, which indicate the fracture front propagation through specimen length. A constant stress region, called the plateau region, is also observed in the quasi-static test results, which is termed as the densification stage. The main reason for the densification stage in the quasi-static tests is the fracture of microballoons. Compressing material consumes the space of microballoons and increases the overall density of the syntactic foam. Microscopic evidences will be sought in the later sections to determine if the same kind of phenomena occurs in high strain rate tests.

The strain rate dependence of peak stress for various types of foams can be observed in Fig. 6. Almost twofold increase in peak stress values is attained at the strain rates of about 1700 $s^{-1}$ compared to quasi-static value in all types of syntactic foams. The increase in maximum strength with increase in strain rate can

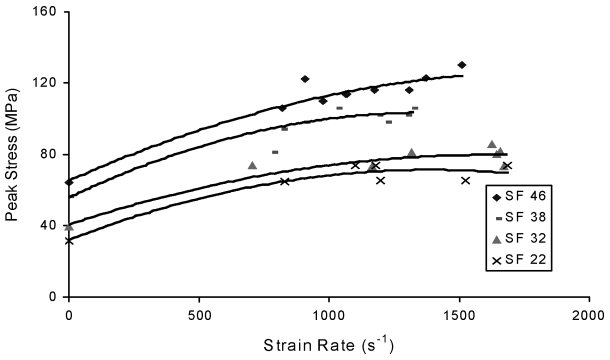


*Figure 6* Peak Stress values for syntactic foams of various densities at different strain rates.

be attributed to the fact that at slower strain rates, the damage propagates more slowly expending most of the applied energy. However, at higher strain rates, the damage does not have enough time to propagate and thus a higher amount of energy is absorbed under this situation. This is accomplished by increase in stress level as compared to quasi-static conditions for similar strain values. Additionally, viscoelastic nature of the polymer matrix itself is responsible in addition to the time dependent nature of damage accumulation. Another observation from Fig. 6 indicates that similar to quasi-static testing, the maximum stress values increase with increasing syntactic foam density. The peak stress is calculated to be 130.8 MPa for the SF46 foam having density value of 460 kg/m$^3$ and progressively decreases with decrease in density and becomes about 65.4 MPa for SF22 syntactic foam having density value of 205 kg/m$^3$.

It is possible to consider the combined effect of strain rate and density of the syntactic foam on peak stress values in different strain rate ranges. Fig. 6 shows almost linear increase in peak stress values with increasing strain rates for higher density syntactic foams (SF46 and SF38). For lower density foams, this increase is linear up to the strain rates of about 1100 s$^{-1}$ and then it becomes nonlinear where the curves become almost flat. This phenomenon is more apparent from Fig. 7 where with increasing strain rate, lower density forms show relatively less increase in peak stress values compared to those of higher density foams. This means that in case of the lower density (higher $\eta$) foams the strain rate sensitivity of peak stress decreases at higher strain rate values where microballoons play a major role in sustaining applied stress. At lower strain rates where matrix failure is more dominant, the peak stress values appear to be almost equally strain rate sensitive regardless of the density of the foam. The variation in strain rate sensitivity of the syntactic foams in different strain rate regions will become clear in the section on failure mechanisms of foams where it can be found out that the mode of failure is the determining factor for strain rate sensitivity.

Crushing of microballoons is a considerably important mechanism of failure for lower density syntactic foams under quasi-static conditions of loading. Significantly high failure strains can be expected in this case due to the availability of newly created space by breaking of hollow microballoons. With increase in density of syntactic foam, vertical crack originated under lateral secondary tensile stresses limits the total strain in the materials before its failure. Therefore, lower failure strain can be expected. These phenomena are quite clear from Fig. 8. It can be observed that under quasi-static loading, the failure strain decreases considerably from 9.41% for SF22 to 5.82% for SF46. The failure strain remains almost the same at high strain rate ($\sim$1300 s$^{-1}$) for higher density syntactic foams but the gap between failure strains at quasi-static and high strain rate increases considerably at lower densities of the foam. Thus it can be inferred that under dynamic conditions of loading, lower density foams are more susceptible to vertical cracking of the materials than crushing of microballoons. In general increasing trend of failure strain with decreasing density of the syntactic foam becomes less and less prevalent with increased strain rates.

Fig. 9 shows stress-strain curves for SF38 syntactic foam at various strain rates. It can be observed that stress-strain curves get stiffened significantly at higher strain rates compared to the static curve due to viscoelastic nature of the polymer matrix. Similar trends are observed for all types of foams. Compressive modulus values for all types of foams at various strain rates are presented in Table III. An appreciable amount of increase in modulus values is observed for all kinds of foams with increase in the strain rate. At the strain rates of about 1700 s$^{-1}$ up to 37% increase has been noted in the modulus as compared to quasi-static value. It is interesting to note two facts here. First, the volume fraction of the polymer matrix is the same for each type

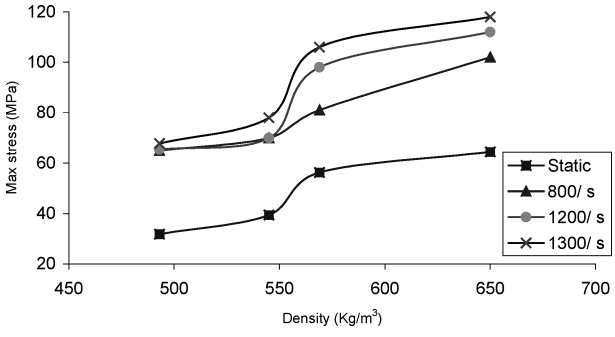


*Figure 7* Syntactic foam density dependence of maximum stress at various strain rates.

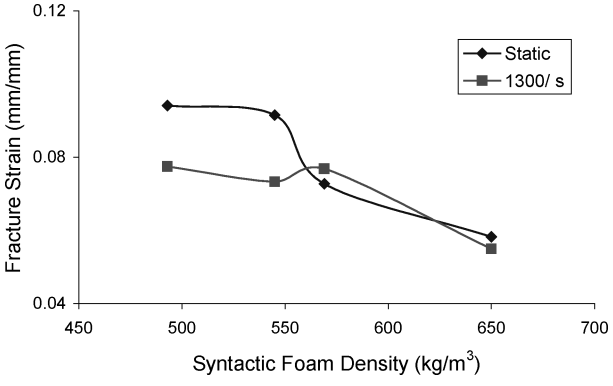


*Figure 8* Fracture strain values for various foam densities at different strain rates.

TABLE III. Change in modulus with strain rate

| Syntactic foam type | Strain rate ($s^{-1}$) | Modulus E (MPa) | Percentage change |
|---|---|---|---|
| SF 22 | Static | 1547 | - |
| | 830 | 1777 | 14.86 |
| | 1200 | 1969 | 27.77 |
| | 1688 | 2503 | 37.29 |
| SF 32 | Static | 2025 | – |
| | 703 | 2191 | 8.19 |
| | 1164 | 2372 | 17.13 |
| | 1636 | 2601 | 28.44 |
| SF 38 | Static | 2394 | – |
| | 830 | 2796 | 16.79 |
| | 1030 | 2888 | 20.63 |
| | 1324 | 1864 | 19.65 |
| SF 46 | Static | 2639 | – |
| | 979 | 3132 | 18.68 |
| | 1015 | 3161 | 19.78 |
| | 1460 | 3564 | 35.20 |

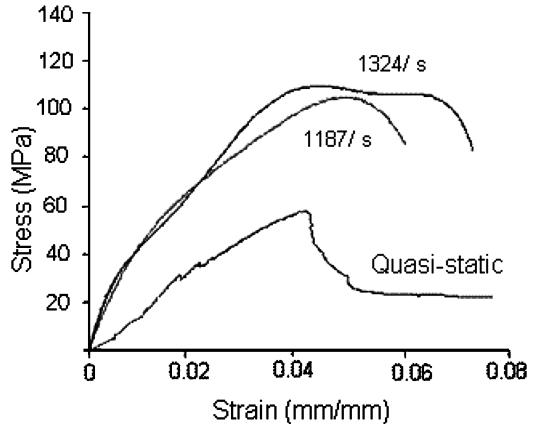


*Figure 9* Static and dynamic stress-strain curves for SF38 specimens.

of foam. Second, for all types of foams the percentage changes in the elastic modulus values at any similar higher strain rates compared to respective quasi-static values are almost the same. Hence, it can be concluded that elastic modulus variation is due to the matrix part of foam only and not due to microballoons.

## 5.2. Failure observations

In the quasi-static compression tests of syntactic foams it is observed that the specimen failure takes place under the combined effects of shear and secondary tensile stresses as shown in Fig. 10. Specimen of SF38 syntactic foam is shown in this figure. Shear cracks originate from the corners of the specimens and propagate at 40–60 ° angles. Cracks originated under lateral secondary tensile stress are in the direction of applied load. It is noticed that as the foam density increases, vertical splitting becomes more and more prominent. Also initiation of the crack is highly influenced by the stiffness of the material. Higher stiffness syntactic foams, with higher density (lower microballoon $\eta$), show early formation of the vertical crack. On the contrary, the foams with lower density (higher microballoons $\eta$) show higher strains before origination of vertical crack and final failure of the specimen. The higher specimen failure strain also leads to more crushing of microballoons in the syntactic foams.

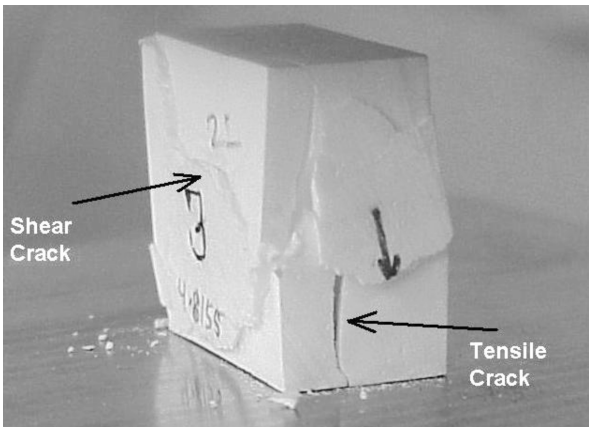


*Figure 10* Optical micrograph of a SF38 syntactic foam specimen failed under quasi-static testing in mixed failure in shear and vertical splitting.

Failure modes of specimens tested at high strain rate are evaluated using optical and scanning electron microscopy. Although the stress-strain responses of the individual category of syntactic foam specimen portray some unique characteristics, the samples share some common modes of failure for all kind of foams.

In high strain rate test specimens crack starts from one end and propagates to the other end across the specimen length. It initiates with two shear planes originating from the edges of the same end of cylindrical specimen. Under the effect of secondary tensile stresses these shear planes eventually join together and form a crack plane along the length of the specimen. Optical micrograph showing this mode of failure is shown in Fig. 11. Substantial amount of damage is noticed at this end of specimen and on the shear planes caused by crushing of microballoons. Debris of microballoons at this specimen end is visible all over the micrograph in Fig. 12. This crack then travels through the specimen causing the ultimate fracture. The higher the strain rate, the lower will be the shear failure at the ends and most of the fracture will be a result of straight cleavage like tensile crack plane. A typical example of this kind of fracture is shown in Fig. 13, which shows a SF46 specimen tested at 1680 $s^{-1}$ strain rate. In this figure a straight crack plane is initiated at the incident end

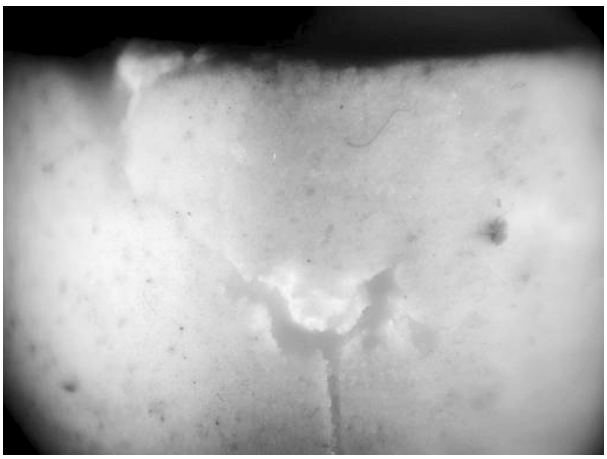

*Figure 11* Optical micrograph of a dynamically tested specimen showing two shear planes originated at the specimen end and then joining together to form a vertical crack.

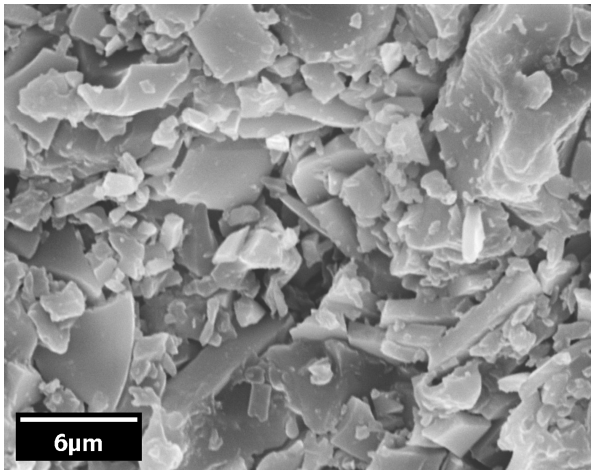


*Figure 12* Debris of crushed microballoons at the end of a specimen.

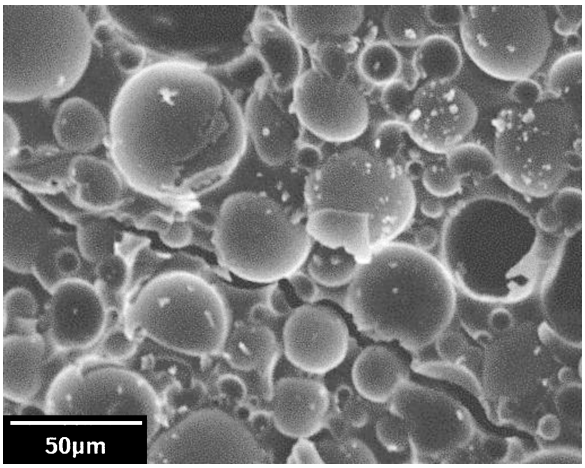


*Figure 14* A low strain rate crack avoids microballoons.

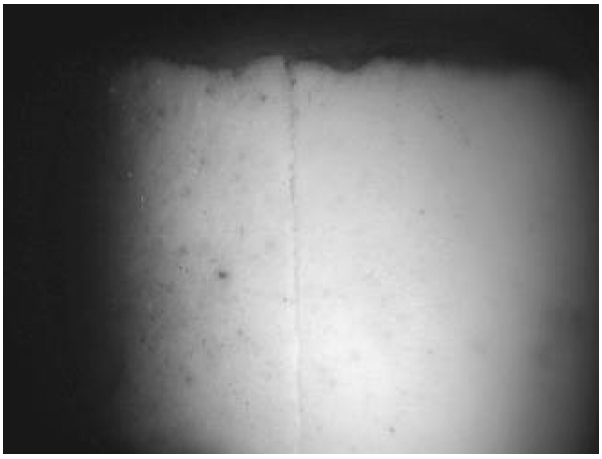

*Figure 13* A crack originated at the specimen end causing vertical splitting in the specimen as observed under optical microscope.

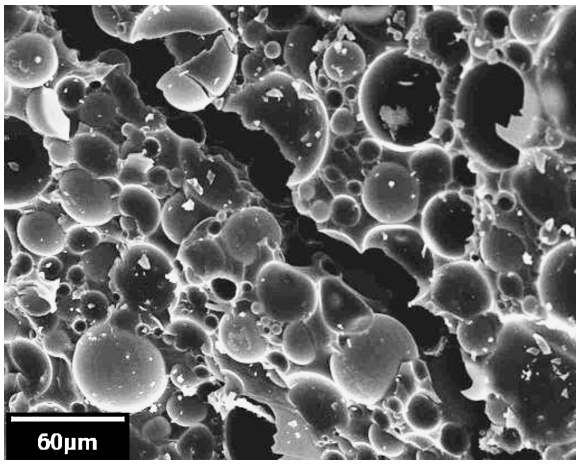


*Figure 15* A crack passing through microballoons under high strain rate conditions.

of the specimen, which eventually propagates to the transmitted end without any deviation.

Although the failure mechanism for high strain rate testing as mentioned above seems similar to the vertical splitting mechanism observed for quasi-static testing of the syntactic foam specimens, scanning electronic micrographic observations reveal some interesting differences. In the lower strain rate test specimens it is observed that the crack propagates through either the matrix material or the matrix-microballoon interfaces as shown in Fig. 14. Crack does not tend to fracture the microballoons and bypasses them completely. In higher strain rate test specimens, crack tends to fracture the microballoons while propagating (Fig. 15). A higher magnification micrograph shows the crack propagation through a microballoon causing its ultimate fracture as shown in Fig. 16. This consumes a higher amount of energy at high strain rates and requires higher amount of stresses for fracture as compared to quasi-static testing. Fig. 17 shows the side view of a failed specimen under dynamic loading. Here, like a typical brittle-like fracture, the fracture plane passes through microballoons and cut them into hollow hemispheres.

In many cases, a network of cracks derived from the original crack plane or from either of the specimen ends or from voids was observed. The voids in the specimen are also found to be "attraction centers" for

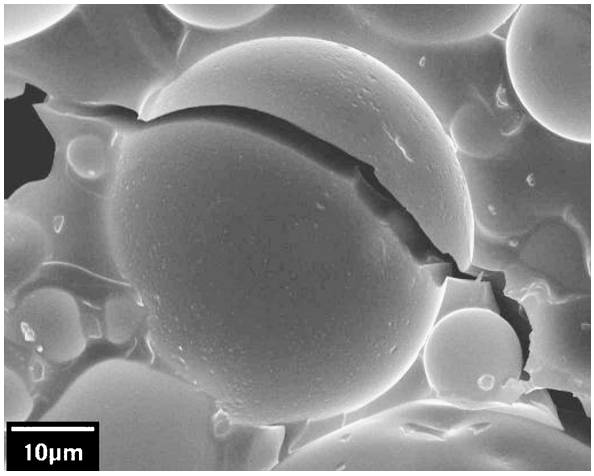


*Figure 16* SEM image of enlarged view of Fig. 15 showing crack's path through a microballoon.

the cracks and cause fracture planes to change their original direction. Fig. 18 shows an SEM image of fracture planes meeting at a void site. Another SEM image in Fig. 19 shows a fracture plane being attracted by a void where its lower wall remains undamaged (central portion of the micrograph). Hence, voids are found to influence crack path and play an important role in deciding the mechanical properties at high strain rates.

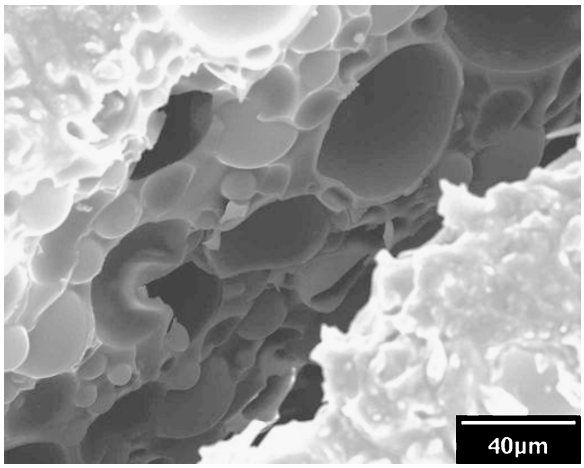


*Figure 17* scanning electronic image showing the crack plane passing through microballoons breaking them into hollow hemispheres.

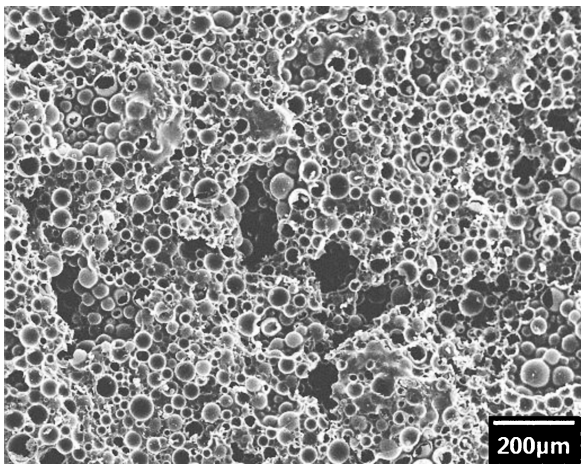


*Figure 18* Crack planes observed to be attracted by higher void density. The planes are observed to change their path due to voids in the material.

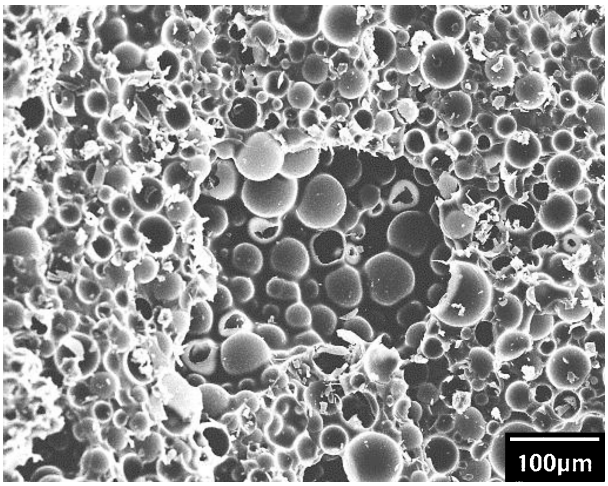


*Figure 19* Fracture surfaces meeting at a void. The lower half of the void can be seen as undamaged group of microballoons in the center of the micrograph.

## 6. Summary

- In contrast to metallic foams, syntactic foams are found to be highly strain rate sensitive. SHPB is found to be an effective and reliable instrument for testing high strain rate properties of syntactic foams.
- Almost twofold increase in the maximum stress is observed for the samples tested at a strain rate of about 1700 $s^{-1}$ as compared to the quasi-static value. The strain rate sensitivity of the maximum stress is found to vary with density of the foam and the strain rate range.
- Strain at maximum stress is found to be almost constant for foams containing all types of microballoons. The failure strain values are observed to increase with increasing microballoon internal radius. Strain rate sensitivity of failure strain for syntactic foam depends on the density of the foam and the applied strain rate.
- Continuous increase in modulus unlike metallic foams is obtained with increasing strain rate due to viscoelastic nature of polymeric matrix.
- Failure initiated by shear at one end of the specimen is found to propagate along the length of the specimen creating flat fracture surfaces showing its brittle-like characters. The crack does not deviate from its path to avoid the harder microballoons until it causes ultimate fracture of the specimen unlike the one observed under low strain rate conditions.

## Acknowledgments

DOW Chemical Company and 3M are acknowledged for supplying the epoxy resin and microballoons respectively, for the fabrication of syntactic foam. Authors are thankful to Ms. Mary Shanti Pampana for assistance during scanning electron microscopy of the specimens

## References

1. F. A. SHUTOV, "Handbook of Polymeric Foams and Foam Technology" (Hanser Publishers, New York, 1991) p. 355.
2. K. ASHIDA, "Handbook of Plastic Foams: Types, Properties, Manufacture and Applications" (Noyes Publications, New Jersey, 1995) p. 147.
3. N. GUPTA and E. WOLDESENBET, *Composite Structures* **61**(4) (2003) 311.
4. C. S. KARTHIKEYAN, KISHORE and S. SANKARAN, *J. Reinf. Plast. Compos.* **20**(11) (2001) 982.
5. A. K. NOOR, W. S. BURTON and C. W. BERT, *Appl. Mech. Rev.* **49**(3) (1996) 155.
6. N. GUPTA, KSHORE, E. WOLDESENBET and S. SANKARAN, *J. Mater. Sci.* **36**(18) (2001) 4485.
7. N. GUPTA, E. WOLDESENBET and KISHORE, *J. Mater. Sci.* **37**(15) (2002) 3199.
8. C. S. KARTHIKEYAN, S. SANKARAN, M. N. JAGDISH KUMAR and KISHORE, *J. Appl. Poly. Sci.* **81** (2001) 405.
9. E. RIZZI, E. PAPA and A. CORIGLIANO, *Int. J. Solids Struct.* **37** (2000) 5773.
10. J. R. M. D'ALMEIDA, *Compos. Sci. Technol.* **59** (1999) 2087.
11. P. BUNN and J.T. MOTTRAM, *Composites* **24**(7) (1993) 565.
12. N. GUPTA and E. WOLDESENBET, *Composites Part A* **35**(1) (2004) 103.
13. M. NARKIS, S. KENIG and M. PUTERMAN, *Polym. Compos.* **5**(2) (1984) 159.
14. R. C. PROGELHOF, in Proceedings of Instrumented Impact Testing of Plastics and Composite Materials (Houston, March 1986) (ASTM) p. 105.
15. D. F. SOUNIK, P. GANSEN, J. L CLEMONS and J. W. LIDDLE, *J. Mater. Manuf.* **106**(5) (1997) 211.
16. W. HALL, M. GUDEN and C. J. YU, *Scripta Mater.* **34** (2000) 515.

17. A. DANNEMANN and J. LANKFORD, *Mater. Sci Eng.* **A293** (2000) 157.
18. T. MUKAI, H. KANAHASHI, T. MIYOSHI, M. MABUCHI, T. G. NIEH and K. HIGASHI, *Scripta Materialia* **40**(8) (1999) 921.
19. V. S. DESHPANDE and N. A. FLECK, *Int. J. Impact Engng.* **24**(3) (2000) 277.
20. W. CHEN, F. LU and N. WINFREE, *Exper. Mech.* **42**(1) (2002) 62.
21. A. RINDE and K. G. HOGE, *J. Appl. Polym. Sci.* **15** (1971) 1377.
22. W. E. BAKER, T. C. TOGAMI and J. C. WEIDER, *Int. J. Impact Eng.* **21**(3) (1998) 149.
23. H. ZHAO and G. GARY, *ibid.* **21** (10) (1998) 827.
24. B. SONG, W. CHEN and D. J. FREW, *J. Compos. Mater.* **38**(11) (2004) 915.
25. B. SONG, W. CHEN, T. YANAGITA and D. J. FREW, *Comp. Struct.* **67** (2005) 289.
26. N. GUPTA and E. WOLDESENBET, in Proceedings of 16th Annual Technical Conference of the American Society for Composites Proceedings (Blacksburg, VA, September, 2001), paper #055.
27. N. GUPTA and E. WOLDESENBET, in Proceedings of 17th Annual Technical Conference of the American Society for Composites (Lafayette, IN, September, 2002), Paper # 042.
28. H. KOLSKY, *Proc. Phys. Soc.* **B62** (1949) 676.
29. A. KAISER, A. WICKS, L. WILSON and W. SAUNDERS, Thesis Submitted to Virginia Polytechnic Institute and State University, Blacksburg, Virginia (1998) 1–84.
30. T. YONEYAMA, H. DOI, E. KOBAYASHI and H. HAMANAKA, *J. Mater. Sci.* **11** (2000) 333.
31. A. JADHAV, E. WOLDESENBET and S. S. PANG, *Composites Part B* **34**(4) (2003) 339.

*Received 14 May 2003*
*and accepted 16 February 2005*